Dry deposition of atmospheric aerosols: Approaches, observations and mechanisms

Delphine K. Farmer*, Erin K. Boedicker and Holly DeBolt

Department of Chemistry, Colorado State University, Fort Collins, CO 80523

ORCID IDs

Delphine Farmer: 0000-0002-6470-9970

Erin Boedicker: 0000-0002-4441-3312

Holly DeBolt: 0000-0002-5643-8015

*Corresponding Author: D. Farmer, delphine.farmer@colostate.edu, (970)491-0624

Keywords: aerosol, particle, dry deposition, flux

Running title: Dry deposition of atmospheric particles

Abstract.

Aerosols are liquid or solid particles suspended in the atmosphere, typically with diameters on the order of nanometers to microns. These particles impact air quality and the radiative balance of the planet. Dry deposition is a key removal process for aerosols from the atmosphere, and plays an important role in controlling the lifetime of atmospheric aerosols. Dry deposition is driven by turbulence, and shows a strong dependence on particle size. This review summarizes the mechanisms behind aerosol dry deposition, including measurement approaches, field observations, and modeling studies. We identify several gaps in the literature, including deposition over the cryosphere (i.e. snow and ice surfaces) and the ocean – and highlight measurement opportunities with new techniques to measure black carbon fluxes. While recent advances in aerosol instrumentation have enhanced our understanding of aerosol sources and chemistry, dry deposition and other loss processes remain poorly investigated.

1. Introduction

Aerosols are the strongest driver of uncertainties in understanding human impacts on climate.(1; 2) Aerosols are small particles, either liquid or solid, suspended in the atmosphere. These particles directly interact with light through scattering (thereby having a cooling impact in the atmosphere, the extent of which depends on particle size) and absorption (thereby warming the atmosphere if the particle composition has adequate chromophores, typically through ‘brown’ and ‘black’ carbon). However, particles can also have indirect impacts on the atmosphere’s radiative balance by their interactions with water vapor in the atmosphere and growth into cloud droplets. Cloud droplets scatter light and enhance the albedo of the planet, and anthropogenic

particles tend to enhance the albedo of clouds. The physical size and chemical properties of atmospheric aerosol particles determine their potential to influence the radiative balance of the planet. These properties are not static: atmospheric chemistry can change the chemical and physical properties of aerosol particles. Gas-particle partitioning, coagulation with other particles, and chemical reactions on particle surfaces can all enable changes in composition and chemical properties, including hygroscopicity, volatility and viscosity. All the different ways that aerosol affects climate, however, depend on their concentrations, which itself depends strongly on their removal rates. Thus, while these aerosol-cloud-radiation interactions are complex, it is the removal of these particles from the atmosphere that represents the single largest uncertainty in climate.(3; 4) Here, we build on previous work (5-8), and review the literature on dry deposition of particles from the atmosphere to surfaces, with particular emphasis on particle deposition measurements in the sub-micron size range over different surface types.

1.1 Particle lifetime

Particles are removed from the atmosphere through wet and dry deposition, both of which are typically considered true sinks (Figure 1). Dry deposition refers to the removal of particles by collision with terrestrial or hydrological surfaces by gravitational settling, impaction, interception and/or diffusion (Figure 2). Wet deposition refers to the scavenging of particles from the atmosphere by solid or liquid water and subsequent removal by precipitation. One nuance in this definition of wet deposition is that cloud droplets can subsequently evaporate and release the particles back into the atmosphere, albeit after potentially substantial aqueous chemical processing. As a result of wet and dry deposition, the lifetime of submicron particles is typically

considered about a week in the atmosphere - long enough for intercontinental transport. On a global scale, this lifetime is dominated by wet deposition, but dry deposition is an important lever on aerosol lifetime in the absence of precipitation.

Presently, there are serious problems with the existing understanding of depositions rates: current parameterizations are inaccurate (9-14); measurements are scarce; and, as expected, the rates are very important. For example, Goldstein and Galbally (15) estimated that wet deposition of secondary organic aerosol (one type of aerosol) was about 4 times that of dry deposition , but that the uncertainties in organic aerosol lifetime due to deposition were substantial. As the atmospheric relevance of aerosol-phase reactions are often assessed by comparison of reaction rates versus aerosol lifetimes, this uncertainty in deposition rates also impacts the way we think about aerosol chemical reactivity.

The relative importance of these dry deposition processes depends on particle size, with gravitational settling significantly impacting only larger (i.e. >10 μm in diameter) particles, and diffusion acting on only the smaller (<300 nm) particles.(16) Dry deposition is typically described by the concentration (C) of the species of interest and a deposition velocity, V_{dep}:

$$Deposition\ Flux = -V_{dep} \times C \quad (1)$$

V_{dep} is expressed as a rate; for submicron aerosol particles, V_{dep} are typically on the order of 0.1 cm/s. A downward flux, or deposition, is taken as a negative flux by convention, while an upward or emitting flux is positive. V_{dep} provides a particularly useful metric for comparing results across sites – and for modeling particle removal – because it is independent of ambient concentration. Observation techniques typically measure the flux and concentration of particles,

and derive the V_{dep}. However, dry deposition is challenging to measure because most measurement techniques rely on micrometeorological techniques, which require careful site selection and either vertical gradients in concentration (difficult as differences in actual concentration may be on par or smaller than differences in inlet losses) or particularly fast, sensitive and selective detectors for eddy covariance flux measurement (Section 2).

The V_{dep} of particles can be directly related to the lifetime of aerosols due to dry deposition:

$$\tau_{dry\ dep} = \frac{V_{dep}}{BLH} \quad (2)$$

where BLH is the boundary layer height (typical afternoon BLH in troposphere are 1-3 km). The total atmospheric lifetime of particles is determined by dry and wet deposition. However, atmospheric chemists rarely consider total particle concentration, and instead often consider particles of specific sizes. In these cases, the lifetime of particles will additionally depend on removal rates of particles from the size range of interest through coagulation or condensation (resulting in particle growth). Particles are less likely to shatter in the atmosphere, though particles can shrink due to evaporation.

1.2 Particle deposition as a key uncertainty in climate models

While there are many reasons for the uncertainty in the aerosol impact on climate, they fundamentally stem from our ability to represent the processes that shape the size and concentration of particles in the atmosphere, including aerosol sources and sinks. Lee et al.(4) found uncertainty in dry deposition velocities of particles in the accumulation mode to be the largest contributor to uncertainty in cloud condensation nuclei (CCN) concentration in global

models, which is critical to understanding cloud interactions (4). CCN are the particles to which water vapor condenses in the atmosphere and form cloud droplets. CCN can have varying compositions and sources, and we point the reader to several reviews that summarize the chemistry and physics of CCN (17; 18). CCN are typically sub-micron in diameter, but the deposition rates of larger particles are also relevant to climate processes - including dust (100 nm to 100 um in size). CCN. Similarly, Carslaw et al.(2) found dry deposition of accumulation mode particles to be the largest contributor to uncertainties in the cloud albedo aerosol indirect effect.

Dry deposition parameterizations are important to get right. Lee et al.(4) used expert elicitation to determine plausible ranges for 28 uncertain inputs to global aerosol microphysics models, including dry deposition of Aitken (0.01 – 0.1 μm in diameter) and accumulation mode (typically 0.1 – 1 μm in diameter) particles. The purpose of this study was to determine the model inputs that contribute most to uncertainties in CCN predictions, both globally and regionally. Lee et al.(4) found dry deposition of particles in the accumulation mode to be the largest individual contributor to uncertainty in CCN – and Aitken mode dry deposition to be the ninth most important contributor. The maximum absolute uncertainties in CCN due to dry deposition occur over land where aerosol concentrations are highest. The maximum relative CCN uncertainties occur over remote regions, and are due to instances where dry deposition is the sole removal mechanism for air masses over timescales of several days. Uncertainties in size-dependent aerosol dry deposition rates dominate CCN prediction uncertainties over remote regions, particularly in regions with low precipitation rates.

In a parallel study, Carslaw et al.(2) found dry deposition of accumulation mode particles to be the largest aerosol process contributor to uncertainties in the cloud albedo aerosol indirect effect. The bounding range for Aitken mode aerosol deposition was 0.5-2x the best guess (scaled evenly around the globe), while the bounding range for accumulation mode deposition was 0.1-10x the best-guess values. These uncertainty ranges reflect uncertainties in both the dry deposition parameterizations themselves (16; 19), and the uncertainties in the variability of subgrid-scale deposition rates. The large uncertainty range for the accumulation mode particles is due to the more parameterized nature of the deposition of these particles, as opposed to the relatively well-understood Brownian diffusion of the smaller, Aitken mode particles (20).

The results of Carslaw, Lee and co-workers strongly emphasize the need for increased certainty in accumulation mode aerosol dry deposition rates. The spatial distribution of these relative CCN uncertainties (proportional to aerosol indirect effect uncertainties) are particularly intriguing. Remote ocean surfaces also remain among the most logistically challenging environments to conduct field measurements over. Further, measurements over water surfaces are inherently challenged by the competition between deposition processes and simultaneous emission of sea spray aerosol due to wave-breaking.

1.3 Particles as a source of nutrients and pollutants to ecosystems

While wet and dry deposition processes obviously remove particles from the atmosphere, mass is conserved: these processes that act as sinks from the atmosphere are also sources to Earth's terrestrial and aquatic surfaces. Addition of acidic compounds, including sulfuric acid / sulfate ions and nitric acid / nitrate ions have been the focus of decades of research into acid deposition

to ecosystems. The addition of acidic components through atmospheric deposition can have devastating consequences to ecosystems including shifts in biodiversity, diminished plant health and damage to aquatic life.(21) Deposition of nitrogen compounds has been an additional focus in terrestrial ecosystems as nitrogen is often a limiting nutrient in temperature forests and agricultural systems.(22) Aerosols are often an important source of this deposition to natural ecosystems, although their impact on crops is potentially small (23). For example, one study in the Netherlands suggested that aerosol deposition accounts for 9% of total nitrate (NO_3^-) and 11% of ammonium (NH_4^+) deposition over the entire country – but the relative contribution approximately doubled over forests, accounting for 20% of NO_3^- and 17% of NH_4^+ deposition over coniferous forests.(24) Phosphorus is an intriguing element in terms of aerosol deposition: while there are few measurements of aerosol phosphate deposition, Vicars et al. (25) showed that deposition of aerosol phosphorus was significant to ecosystems in the Sierra Nevada, potentially leading to phytoplankton growth and eutrophication in lakes. We point readers to recent reviews for detailed analysis of long-term trends and consequences of atmospheric deposition from an ecosystem perspective. (26) Deposition of particles containing toxic metals, pesticides, polyflourinated compounds, or persistent organic pollutants are emerging topics of concern.(27-29) Thus, a mechanistic understanding of particle deposition is essential not only for understanding the lifetime of aerosols in the atmosphere, but also for determining the addition of pollutants and nutrients from the atmosphere to terrestrial and aquatic ecosystems.

2. Particle Deposition Measurement Approaches

Our capacity to accurately parameterize dry deposition and thus model particle lifetimes in the atmosphere is limited by the small number of observations of particle fluxes. While measuring particle number concentrations, size distributions and composition is relatively straight-forward(30), flux measurements are not. Measurements of the surface-atmosphere exchange of particles – particularly in remote, low-concentration regions – have been elusive.

Multiple techniques have been used for measuring particle fluxes over surfaces, including the use of wind tunnels in laboratory experiments (31), but micrometeorological techniques (32) have emerged recently in the literature as preferred techniques. Pryor et al (33) provides a rigorous analysis of these micrometeorological techniques, so we only briefly summarize them below.

The eddy covariance (EC) method is the most direct micrometeorological technique used for determining the vertical turbulent flux and exchange rate of particles over a given ecosystem.(33) The EC technique measures surface-atmosphere exchange, or flux (F), by averaging the deviations from the mean of vertical wind speed (w') and concentration (c'), typically over 30 minutes (32; 34):

$$F = \langle w'c' \rangle \qquad (3)$$

Concentration may be taken as aerosol number or mass within a chosen size bin. This approach requires measurements of vertical wind speed (typically by a sonic anemometer) and particle concentration (typically measured by fast optical sensors, either as a size-resolved value, or as an integrated sum of particles within the inlet/instrument sampling range). EC requires fast data acquisition (typically >5 Hz) and the appropriate physical location for sampling. Historically, individual condensation particle counters with known size cuts (35) were used to calculate

particle fluxes. More recently, the instrument requirements are often met with rapid optical measurement techniques – often home-built or modified commercial instrumentation (11), although some more recently available commercial analyzers are capable of size-resolved particle flux measurements (12; 36). Mass spectrometry-based instruments can provide chemical resolution, but are typically unable to provide rapid size-resolution.(37; 38) The choice of sampling location must reflect several important assumptions. Measurements must be representative of an upwind area and within the boundary layer of interest to ensure that the 'fetch' (i.e. area over which measurements are being integrated) is adequate. The terrain must be horizontal and uniform, and the flux must be fully turbulent (i.e. most of the vertical transfer must be done by eddies). Meeting these requirements is challenging, as exemplified in studies over high roughness terrains. (39)

Alternate micrometeorological techniques for size-resolved particle fluxes include the relaxed eddy accumulation (REA) technique, which enables slower detection techniques by separately sampling drafts in the upward versus downward (and, ideally, neutral) directions.(40) REA measurements of size-resolved particles have been successfully implemented over several forest sites,(41; 42) and often provide comparable results to eddy covariance approaches.(43) Several groups have also successfully deployed disjunct sampling techniques.(44) For example, Held et al. (45) applied single particle time-of-flight mass spectrometry to the disjunct eddy sampling to derive chemically resolved particle fluxes, but noted that the required data processing was substantial.

The gradient approach is simpler still, with measurements at fixed heights along a vertical gradient coupled to sonic anemometers, thus enabling users to derive vertical fluxes. This

approach holds many assumptions regarding turbulence conditions, and requires the measurements at different heights to be comparable. Aerosol particles have size-dependent losses in inlet lines and are subject to gas-particle partitioning – thus making gradient measurements with different inlet lengths (or bends in inlet lines if identical in length) particularly challenging.

An indirect approach to quantifying dry deposition to surfaces is to collect particles deposited to proxy surfaces. However, these approaches are limited in the ability of proxy surfaces to both physically and chemically represent true ecosystem surfaces, the potential for deposited particles to change form or evaporate after deposition, and the inability of analytical techniques to resolve whether observed compounds deposited on surfaces truly deposited as particles rather than gases. Large monitoring networks have successfully established measurements of particle deposition of specific chemical components (e.g. NO_3^-, SO_4^{2-}, NH_4^+), but these measurements do not typically separate deposited aerosol by size, and thus do not provide size-resolved flux information.

2.1 Challenges in interpreting observed fluxes

Even when all the requirements for micrometeorological flux measurements are met, there are numerous challenges inherent in interpreting observed size-resolved particle fluxes. Model-measurement comparisons typically assume that the aerosol flux measurement is driven entirely by dry deposition. However, particle flux observations often include upward fluxes indicative of source terms from in-canopy chemistry and secondary organic aerosol formation, bioaerosol or other primary emission, gas-particle partitioning along vertical thermal gradients, or in-canopy particle nucleation (5; 46-50). A sink term from deposition must be isolated in order to properly

evaluate deposition models. This idea that chemically-induced fluxes impact observations of deposition for total aerosol has been validated by the observation that the chemical components of aerosols deposit at different rates (20; 37; 51). Black carbon (BC) may provide a useful test of size-resolved dry deposition parameterizations as it is not subject to the chemical interferences inherent to total aerosol flux measurements. Aerosol number measurements have significant contributions of organic aerosol and other chemical components subject to gas-particle partitioning or oxidation chemistry, while BC does not undergo significant chemical change on the timescale of turbulent eddies (<15 minutes), and should be unaffected by these otherwise confounding processes.

Humidity poses an additional challenge in interpreting observed size-resolved particle fluxes. Particles typically contain water in the ambient air, depending on their size, hygroscopicity, and the ambient relative humidity. Our fundamental understanding of the factors that control turbulent motion or gravitational settling of particles in the atmosphere is that these factors are influenced by the actual size of the particles. Thus when measuring the size-dependent particle flux (i.e. the correlation between particle number concentration and vertical wind speed), the sizing of particles may be easier to interpret when the particle is wet, not dry. This nuance is counter to many aerosol measurement approaches, in which ambient particles are typically dried before sizing. Vertical gradients in temperature or concentration can similarly cause shifts in aerosol size distribution on the timescales of vertical exchange.(51; 52)

3. Observations of particle deposition

There are few recent measurements of aerosol flux, and thus V_{dep} observations, over vegetated surfaces. This lack of observations is dominantly due to the challenges with aerosol flux measurements. While there are reviews of particle flux and deposition measurements, it has been over a decade since a comprehensive report of all current measurements - for all types of ecosystems - has been attempted (5; 53), although we note the recent work of Saylor et al (13),Petroff and colleagues (54), and Emerson et al (14). In Table 1, we compile an extensive list of dry deposition particle measurements, including the studies that report deposition velocities along with information about measurement size range, method, and location. The table is organized first by general land type, grass, forest, water, and snow/ ice, and then by date. A selection of this available data is plotted in Figure 3 to provide a clear, visual representation of gaps in our observations. Here, these observations are used to understand the major questions still facing the study of aerosol dry deposition. Figure 3 highlights the lack of measurements over the cryosphere – and that the bulk of size-resolved particle flux measurements have been collected in the accumulation mode.

Size is clearly a key controlling variable in particle dry deposition (14; 53; 55). Small particles are more strongly influenced by deposition processes driven by Brownian diffusion, while larger particles are more strongly influenced by interception, impaction and gravitational settling (Figure 2). As a result of these competing processes, described in detail in Section 4, deposition velocity typically exhibits a minima in the accumulation mode. This minima occurs because uptake to surface collectors due to Brownian diffusion decreases as size increases, while removal by gravitational settling increase with size. The roles of surface uptake due to impaction and interception processes also increase with size, though models suggest a drop-off at very large (i.e. 10s of μm in diameter) size range. Of course, the relevance of different aerosol modes, or

size ranges, depends on the question being posed: small particles are typically greater in number, but can be less important in terms of mass exchange.

Deposition velocities are clearly a function of turbulence (typically described by friction velocity, u*) – with more turbulent conditions inducing a stronger flux.(11; 36; 56; 57) Land use type also impacts deposition velocity, with more complex ecosystems with greater surface area holding more 'collectors' and enabling more deposition through interception. Hence, deposition velocities over forests are typically greater than over grasslands, which are in turn greater than lakes or smooth aquatic surfaces. At larger particle sizes (>10 μm diameter), gravitational settling plays a controlling role, and deposition rates tend to converge independent of surface structure.

4. Current models and our mechanistic understanding

One major challenge in modeling aerosol concentrations is the prediction of deposition trends over a wide range of land use types, while maintaining model ability to be assimilated easily into global transport and climate models. Models typically use an aerosol deposition module with a particle size dependent resistance approach tailored for terrestrial surfaces (7; 58). Slinn (16) developed a resistance approach to model deposition to various vegetative canopies, utilizing land-use specific resistances. The parameterization developed by Zhang et al. (19) expanded on the Slinn approach by incorporating simple empirical parameterizations for the dry deposition processes. Zhang et al.(19) also expanded the application of the resistance approach to 14 different land use types, which include water and ice surfaces.

The Zhang framework is currently used in multiple chemical transport and climate models (including GLOMAP and GEOS-Chem). Both Slinn (16) and Zhang et al. (19) describe the particle size-dependent deposition velocity (V_{dep}) as:

$$V_{dep} = V_g + \frac{1}{R_a + R_s} \quad (4)$$

where V_g is the gravitational settling speed, which is a function of particle density, diameter, viscosity of air, and a correction factor for small particles derived from the mean free path of molecules in air, temperature, pressure and kinematic viscosity. R_a and R_s are the aerodynamic and quasi-laminar sublayer resistances, respectively:

$$R_a = \frac{\ln(z_r, z_o) - \Psi_H}{\kappa u_*} \quad (5)$$

$$R_s = \frac{1}{\varepsilon_o u_* (E_B + E_{IN} + E_{IM}) R_i} \quad (6)$$

where z_r is the height, z_o is the roughness length, Ψ_H is the stability function, κ is the von Karman constant and u_* is the friction velocity. In the quasi-laminar sublayer equation, ε_o is an empirical constant, R_i represents the fraction of particles stuck to a surface, and E_B, E_{IN} and E_{IM} are the collection efficiencies of Brownian diffusion, interception and impaction, respectively. Zhang et al. (19) take E_B, and E_{IN} from Slinn (16), and E_{IM} from Peters and Eiden (59):

$$E_B = Sc^{-\gamma} \quad (7)$$

$$E_{IN} = \frac{1}{2}\left(\frac{D_p}{A}\right)^2 \quad (8)$$

$$E_{IM} = \left(\frac{St}{\alpha + St}\right)^{\beta} \quad (9)$$

where *Sc* is the Schmidt number, and *St* is the Stokes number (calculated from gravitational deposition velocity, friction velocity, and either the kinematic viscosity of air for oceans and other smooth surfaces, or the acceleration due to gravity and a 'characteristic radius' that depends on the collection surface, *A*). The other four variables represented in these equations are land use dependent constants for the collection efficiencies: γ (Brownian diffusion), A (interception), α (impaction), and β (impaction). Zhang et al. (19) tuned the γ, A, α, and roughness length (z0) variables for each of the 14 land use types employed in the model. The β term was taken to equal 2 for all land use types in Zhang et al. [2001].

Slightly different frameworks for describing aerosol dry deposition also exist (e.g. 60), but are not commonly used in atmospheric chemical transport models. Alternate equations for the collection efficiency of interception (EIN) and impaction (EIM) have been proposed by Slinn (16), Giorgi (61; 62), Pleim and Ran (63), Petroff and Zhang (54) and Emerson et al. (14), but are infrequently incorporated into global models. These alternate parameterizations are rarely evaluated against aerosol observations. In a key piece of work, Saylor et al. (13) implemented several of these deposition algorithms in a regional air quality model, and found that fine particle concentrations varied 5-15% depending on the deposition algorithm – with total deposition varying by over 200%. Emerson et al. (14) implemented a revision of the Zhang parameterization constrained by observations in a chemical transport model, and noted that global surface accumulation mode number concentrations increased by 62% compared to the Zhang parameterization – and thus impacted the aerosol direct and indirect effect substantially. A closer investigation of these algorithms and model-measurement comparison was clearly warranted.

While the values described in Zhang et al. (19) have been compared against some observations over vegetated surfaces, the parameters used to tune modern deposition models to ocean surfaces have not been tested against observations. This is likely due to the lack of aerosol flux observations, and in particular size-resolved aerosol flux measurements, over the ocean – and the fact that these observations include both a source term from sea spray and a sink term from deposition that must be separated in order to properly evaluate the deposition model. Aerosol dry deposition models that are specific for ocean and water surfaces endeavor to address wind speed dependence and processes specific to the marine environment (e.g. 64; 65-69). However, these models are infrequently used in global models.

A more recent model developed by Petroff and Zhang (54) was able to better capture deposition trends over 26 different land use types defined in the work. The Petroff and Zhang parameterizations are more sensitive to surface changes because of the revised form of the deposition velocity that considers the leaf area index (LAI) as well as canopy height. The model also includes the ground bellow the canopy as a surface for deposition. The second major difference between Petroff and Zhang (54) and Zhang et al. (19)(2001), is the parametrization of Brownian diffusion, interception, and inertial impaction as well as the inclusion of turbulent impaction in Petroff and Zhang (2010):

$$E_{IB} = C_B Sc^{\frac{-2}{3}} Re^{-\frac{1}{2}} \quad (10)$$

$$E_{IN} = C_{IN}\left(\frac{dp}{A}\right) \ (needle-like\ obstacles) \quad (11a)$$

$$E_{IN} = C_{IN}\left(\frac{dp}{A}\right)\left[2 + \ln\left(\frac{4A}{dp}\right)\right] \ (leaf\ or\ plane\ obstacles) \quad (11b)$$

$$E_{IM} = C_{IM}\left(\frac{St}{(\alpha+St)}\right)^{\beta} \quad (12)$$

$$E_{IT} = (2.5 \times 10^{-3}) \times C_{IT} \times \left(\tau_{ph}\right)^2 \; if \; \tau_{ph} < 20 \quad (13a)$$

$$E_{IT} = C_{IT} \; if \; \tau_{ph} \geq 20 \quad (13b)$$

where R_e is the Reynolds number on top of the canopy and the C_B, C_{IN}, C_{IM}, and C_{IT} are numerical coefficients for Brownian diffusion, interception, inertial impaction, and turbulent impaction respectively. These constants are adjusted based on the land use type. In equation (11) the τ_{ph} term is the non-dimensional particle relaxation time. Interception deposition efficiency (Equation 11) has two forms, the first is for needle-like obstacles and the second is for leaf or plane obstacles. The β term was also taken to equal 2 for all land use types, just as it was by Zhang et al. (19).

Another important improvement in Petroff and Zhang (54) was the incorporation of velocity attributed to the phoretic effects (V_{phor}) observed over water, ice, and snow surfaces, into the calculation of the drift velocity. This addition significantly increased the accuracy of the predicted size-resolved deposition over these surfaces. When compared to observed deposition measurements for water surfaces, Petroff and Zhang (70) were able to accurately capture the minimum in the deposition trend using the V_{phor} term. For snow and ice surfaces, the improvement is less obvious due to the scarce number of direct deposition measurements over those surfaces to compare the model against.

While the Petroff and Zhang (54) parameterization compares better to observations, it is not currently used in global transport and climate models. One reason for this may be that in Petroff and Zhang (54), a total of 26 land use categories are defined, compared to the 14 originally

incorporated into global models. By changing these fundamental parameterizations, the Petroff and Zhang algorithm may be more difficult to assimilate into current deposition modules than the frequently used Zhang (19)parameterization. Emerson et al (14) aimed to strike a balance between these challenges by maintaining the structure of the key Zhang parameterization, while capturing observed size dependence in dry deposition. It is clear that while a robust parameterization, that agrees well with the available direct deposition measurements, is needed in global models the framework needs to be constrained enough to easily incorporate into a broad array of chemical transport models and into existing deposition modules.

5. Black carbon

Black carbon (BC) is a particularly important material for understanding aerosol lifetime: BC is chemically stable and non-volatile, is only formed in combustion, and can be sensitively and selectively detected, both in the air and post-deposition in the cryosphere. When deposited on snow surfaces, BC increases absorption of sunlight by the surface, enhancing snow aging and melting (71) and generating positive climate feedbacks (72).

Black carbon (BC) directly impacts atmospheric temperature via absorption of solar radiation, and indirectly impacts cloud formation and their optical properties (73). Upon deposition to snow and ice surfaces, BC can alter surface albedo and enhance snowmelt (72; 74). Key BC sources include combustion of fossil fuels and biofuel, and biomass burning and wildfire (75). Major sinks are dry deposition and wet deposition through scavenging by cloud droplets, ice crystals and precipitation. While much recent work has focused on the source, aging and optical

properties of black carbon (e.g. (75) and references therein), the deposition component of the life cycle of BC remains poorly constrained.

BC deposition to snow and ice surfaces links anthropogenic pollution, changes in the planet's radiative balance, and human impacts. Recent work (e.g. (76-79)) has linked BC deposition on snowpacks to more rapid snowmelt and thus the water supply for agriculture and population centers in the Himalaya, Cascades and Sierra Nevada range of California. Hadley et al. (76) noted that atmospheric BC concentrations decreased during snowfall events, suggesting that the bulk of BC that deposited to the Sierra Nevada snowpack was the result of scavenging below clouds rather than ice nucleation. The authors also noted that BC in the Sierra Nevada snowfall would darken fresh snow to such an extent that the albedo could be reduced by >1% (76). In contrast, Yasunari et al. (79) found that dry deposition in the pre-monsoon season of the Himalaya was particularly important for albedo reduction of mountain glaciers, and thus the timing of snowmelt. However, predictions of BC concentrations in snow and their consequent effects on albedo, surface temperatures and snowmelt rely on accurate representations of wet and dry deposition of BC, as well as on the evolution of snow on seasonal timescales (e.g. snow metamorphism, sublimation, melt, blowing). Yasunari et al. (79) noted that “how to estimate [BC dry deposition velocity] more accurately at the grid point, which includes snowcover or glacier surface, is the key to assess[ing] glacier retreats or seasonal snow melt timings, in terms of the debris-covered area, snow darkening effect due to climate and environmental changes, using climate models”. Other work has suggested that wet deposition and transport dominates the lifetime of BC in the Arctic (80), and that more observational constraints on wet deposition in particular are essential. The uncertainties in accurately predicting BC in or on snow surfaces, and

thus the impacts on albedo and snowmelt, are directly linked to the poor understanding of deposition and the lack of BC deposition measurements.

The Single Particle Soot Photometer (SP2; (81; 82)) offers an intriguing opportunity to make eddy covariance surface-atmosphere flux measurements of refractory BC. Emerson et al. (70) demonstrated that this instrument can be coupled to the eddy covariance approach to provide direct flux observations of BC over a grassland, while Joshi et al. (83) demonstrated its flux measurement capacity over the far more polluted urban environment of Beijing.

6. Open questions

Our understanding of size-dependent particle dry deposition is poor due to the lack of field observations. To reduce model uncertainty, we require a deeper understanding of size-dependent dry deposition rates over key terrestrial and aquatic surfaces. Water surfaces and the cryosphere are two particularly poorly understood surfaces for particle dry deposition.

6.1 Water Surfaces

Clouds in the marine boundary layer have a particularly strong, but poorly constrained, influence on climate (84; 85). Clouds are most susceptible to changes due to aerosols when clouds have low optical depths, large horizontal extent, and low aerosol concentrations – as in, for example, the stratocumulus regions of the subtropical oceans (86; 87). Uncertainties in size-dependent aerosol dry deposition rates dominate CCN prediction uncertainties over remote global ocean regions, particularly in regions with low precipitation rates (4). Uncertainties in remote ocean CCN mean that uncertainties in dry deposition could be the leading contributor to uncertainties

in aerosol indirect effects globally due to high cloud susceptibility in many remote ocean regions (2). These results strongly emphasize the need for increased certainty in dry deposition rates over oceans in models (2; 4).

6.2 Cryosphere

Surface properties clearly influence deposition, and while we have developed appropriate parameterizations for dry deposition in forest and grassland ecosystems, we expect the cryosphere to behave as a very different surface for particle uptake due to its distinct chemical and physical properties relative to leaf surfaces.

Direct measurements of dry deposition over ice- and snow-covered surfaces are limited (88-91). Deposition velocities over rough surfaces have been shown to be considerably higher (> 100 %) than those reported over smooth snow-covered surfaces (92). Gallagher et al. (93) observed a similar phenomenon, where the introduction of snowfall to a spruce forest resulted in a two factor reduction in the flux of cloud droplets to the canopy. However, the characteristic size-resolved trend is still present in the data, with ultrafine (<0.1 μm in diameter) and coarse mode (typically, 2.5 – 10 μm diameter) particles depositing faster than accumulation mode particles. Seasonal differences in deposition have also been observed in the cryosphere. Macdonald et al. (94) showed that deposition for accumulation mode black carbon increased during warmer months. This trend is thought to be a result of increased scavenging by mixed-phase clouds during those periods. Measurements with higher size resolution over longer periods are needed to fully understand how these surfaces change particle deposition in the cryosphere.

Accurately characterizing BC dry deposition is particularly important for regions with high snow and ice cover because of BC's high impact on the surface albedo. Huang et al. (95) showed that

alteration of dry deposition parameterizations over the base model was essential for correctly modeling surface concentrations of black carbon in the Arctic; use of an unaltered dry deposition module caused underestimation of surface black carbon by factors of at least 2, and often 5 or more. Huang et al. (95) used the size-resolved resistance-in series approach of Zhang et al. (19). However, to the best of our knowledge, this dry deposition parameterization has never been tested against BC deposition, only total (refractory + non-refractory) aerosol deposition. There is a clear need for an assessment of current deposition models against an observational dataset of aerosol fluxes over the cryosphere.

6.3 Phoretic effects

For water, snow, and ice surfaces there are additional factors impacting particle deposition, in comparison to vegetative surfaces. Near surface gradients in temperature, water vapor, and electricity all have the potential to alter the movement of particles towards the collecting surfaces. These surface effects are collectively referred to as phoretic effects. Thermophoresis, caused by temperature gradients, as well as diffusiophoresis, caused by gradients in water vapor concentration, are both speculated to impact deposition of fine particles. While these phoretic effects can force particle movement towards cold and evaporating surfaces, the Stefan flow effect induces flow towards the condensing surface. The impact of electrophoresis on particle deposition is not well constrained. Tammet et al. (96) investigated these effects through a model study and found them to be an essential mechanism for 10 – 200 nm particles during periods of low wind speed, however, strong wind speeds appear to suppress this mechanism. Full characterization of these effects requires targeted near surface measurements of the magnitude of these gradients.

6.3 Other terrestrial surfaces

The Earth's terrestrial surface is diverse, with different plant structures that will induce different turbulent dependences and different collection efficiences - and thus different deposition rates. Further, plant morphology and physiology is not static, and changes as ecological succession progresses and with seasonal cycles. The role of these changes in surface structure are poorly understood, but may have substantive effects on aerosol dry deposition and thus atmospheric lifetime. For example, Pryor et al. (97) observed enhanced deposition rates for ultrafine (< 100 nm in diameter) particles over a Midwestern US forest during leaf-out relative to bare trees, and were able to attribute the bulk of ultrafine particle deposition to canopy uptake (rather than the ground). In contrast, Rannik and co-workeres (98) made long-term integrated (i.e. not size-segregated) fluxes over a boreal pine forest, and found stronger particle deposition fluxes in the winter than summer – but attributed this seasonal variability to shifts in size distribution, not surface collectors (99).

Urban surfaces are a particularly challenging region to study as airflows and micrometeorology in urban environments are complex. Eddy covariance measurements are challenging and rarely done – although several recent studies have successfully characterized the urban emissions of particles from vehicle exhaust and other sources.(48; 100-104) Deriving the deposition term over urban surfaces is more challenging as it requires measurements far downwind of major sources, or a strong understanding of the simultaneous emissions. However, it is intriguing that deposition has been strong enough over urban parks for several of these studies to observe it.(103; 104)

7. Conclusions

With the exception of urban, ocean, and chemically-resolved particle flux studies, most work to date assumes that observed downward fluxes represent purely deposition processes. However, upward fluxes are frequently observed, whether over forests or grasslands.(46; 97; 105) While such observations are reasonable over urban or marine areas where primary emission sources may be substantial, upward fluxes over remote regions have proven to be more puzzling and often attributed to particle nucleation, entrainment or vertical gradients in gas-particle partitioning. However, Emerson et al.'s recent observation (70) of upward black carbon fluxes over a grassland site suggests that upward fluxes may be ubiquitous and contributing processes, such as resuspension, warrant further investigation.

Dry deposition of particles is an underappreciated uncertainty in our ability to predict both radiative and health effects from atmospheric aerosols. However, newer instruments developed over the past two decades have enabled an array of new field observations of size-resolved particle fluxes. Beyond size-resolution, the addition of chemical-resolution in particle flux measurements would be particularly useful for separating different driving mechanisms responsible for upward and downward fluxes. For example, our 2017 measurements of black carbon wet deposition and surface-atmosphere exchange fluxes over the Southern Great Plains site in Oklahoma allowed us to quantify the relative importance of wet versus dry deposition. In that work, we observed that wet deposition dominated dry deposition at the site during the campaign, resulting in dry deposition accounting for about 6% of the loss and a net lifetime for BC of 7-11 days (70). However, these observations were limited to one location over just a few weeks, and many more measurements over many environments are essential for more generally constraining the importance of, and mechanisms behind, particle dry deposition.

While measurements over terrestrial ecosystems have increased in number over the past two decades, the Earth's surface is complex, and fundamentally improving our understanding of deposition – and thus our capacity to model it – requires additional observations over the cryosphere, water surfaces, urban systems and the biosphere.

Acknowledgements

This work was supported by NOAA's Climate Program Office's Atmospheric Chemistry, Carbon Cycle, and Climate program (grant NA14OAR4310141) and the DOE Office of Biological and Environmental Research (grant DE-SC0016259).

References

1. IPCC IPoCC. 2013. Climate Change 2013 - The physical science basis. Cambridge University Press
2. Carslaw KS, Lee LA, Reddington CL, Pringle K, Rap A, et al. 2013. Large contribution of natural aerosols to uncertainty in indirect forcing. *Nature* 503:67-71
3. Lee LA, Carslaw KS, Pringle KJ, Mann GW. 2012. Mapping the uncertainty in global CCN using emulation. *Atmos Chem Phys* 12:9739-51
4. Lee LA, Pringle KJ, Reddington CL, Mann GW, Stier P, et al. 2013. The magnitude and causes of uncertainty in global model simulations of cloud condensation nuclei. *Atmos Chem Phys* 13:8879–914
5. Pryor SC, Gallagher M, Sievering H, Larsen SE, Barthelmie RJ, et al. 2008. A review of measurement and modelling results of particle atmosphere-surface exchange. *Tellus B* 60:42-75
6. Fowler D, Pilegaard K, Sutton MA, Ambus P, Raivonen M, et al. 2009. Atmospheric composition change: Ecosystems-Atmosphere interactions. *Atmos Environ* 43:5193-267
7. Wesely ML, Hicks BB. 2000. A review of the current status of knowledge on dry deposition. *Atmos Environ* 34:2261-82
8. Ruijrok W, Davidson CI, W. NICHOLSON K. 1995. Dry deposition of particles. *Tellus B* 47:587-601
9. Pryor SC, Barthelmie RJ, Hornsby KE. 2013. Size-resolved particle fluxes and vertical gradients over and in a sparse pine forest. *Aerosol Sci Tech* 47:DOI: 10.1080/02786826.2013.831974
10. Pryor SC, Barthelmie RJ, Spaulding AM, Larsen SE, Petroff A. 2009. Size-resolved fluxes of sub-100-nm particles over forests. *J Geophys Res-Atmos* 114
11. Vong RJ, Vong IJ, Vickers D, Covert DS. 2010. Size-dependent aerosol deposition velocities during BEARPEX' 07. *Atmos Chem Phys* 10:5749-58

12. Petroff A, Murphy J, Thomas S, Geddes J. 2018. Size-resolved aerosol fluxes above a temperate broadleaf forest. *Atmos Environ* 190:359-75
13. Saylor RD, Baker BD, Lee P, Tong D, Pan L, Hicks BB. 2019. The particle dry deposition component of total deposition from air quality models: right, wrong or uncertain? *Tellus B: Chemical and Physical Meteorology* 71:1550324
14. Emerson EW, Hodshire AL, DeBolt HM, Bilsback KR, Pierce JR, et al. 2020. Revisiting particle dry deposition and its role in radiative effect estimates. *Proceedings of the National Academy of Sciences*:202014761
15. Goldstein AH, Galbally IE. 2007. Known and unexplored organic constituents in the earth's atmosphere. *Environ Sci Technol* 41:1514-21
16. Slinn WGN. 1982. Predictions for Particle Deposition to Vegetative Canopies. *Atmos Environ* 16:1785-94
17. Farmer DK, Cappa CD, Kreidenweis SM. 2015. Atmospheric Processes and Their Controlling Influence on Cloud Condensation Nuclei Activity. *Chem Rev* 115:4199-217
18. Poschl U. 2005. Atmospheric aerosols: Composition, transformation, climate and health effects. *Angew Chem Int Edit* 44:7520-40
19. Zhang LM, Gong SL, Padro J, Barrie L. 2001. A size-segregated particle dry deposition scheme for an atmospheric aerosol module. *Atmos Environ* 35:549-60
20. Ruijgrok W, Tieben H, Eisinga P. 1997. The dry deposition of particles to a forest canopy: A comparison of model and experimental results. *Atmos Environ* 31:399-415
21. Stevens CJ, Dise NB, Mountford JO, Gowing DJ. 2004. Impact of nitrogen deposition on the species richness of grasslands. *Science* 303:1876-9
22. Fowler D, Coyle M, Skiba U, Sutton MA, Cape JN, et al. 2013. The global nitrogen cycle in the twenty-first century. *Philos T R Soc B* 368
23. Schiferl LD, Heald CL, Kelly D. 2018. Resource and physiological constraints on global crop production enhancements from atmospheric particulate matter and nitrogen deposition. *Biogeosciences* 15:4301-15
24. Erisman JW, Draaijers G, Duyzer J, Hofschreuder P, VanLeeuwen N, et al. 1997. Particle deposition to forests - Summary of results and application. *Atmos Environ* 31:321-32
25. Vicars WC, Sickman JO, Ziemann PJ. 2010. Atmospheric phosphorus deposition at a montane site: Size distribution, effects of wildfire, and ecological implications. *Atmos Environ* 44:2813-21
26. Bobbink R, Hicks K, Galloway J, Spranger T, Alkemade R, et al. 2010. Global assessment of nitrogen deposition effects on terrestrial plant diversity: a synthesis. *Ecol Appl* 20:30-59
27. Casal P, Zhang Y, Martin JW, Pizarro M, Jiménez B, Dachs J. 2017. Role of Snow Deposition of Perfluoroalkylated Substances at Coastal Livingston Island (Maritime Antarctica). *Environ Sci Technol* 51:8460-70
28. Hageman KJ, Hafner WD, Campbell DH, Jaffe DA, Landers DH, Simonich SLM. 2010. Variability in Pesticide Deposition and Source Contributions to Snowpack in Western US National Parks. *Environ Sci Technol* 44:4452-8
29. Rose NL, Rippey B. 2002. The historical record of PAH, PCB, trace metal and fly-ash particle deposition at a remote lake in north-west Scotland. *Environmental pollution* 117:121-32
30. McMurry PH. 2000. A review of atmospheric aerosol measurements. *Atmos Environ* 34:1959-99
31. Zufall MJ, Dai WP, Davidson CI. 1999. Dry deposition of particles to wave surfaces: II. Wind tunnel experiments. *Atmos Environ* 33:4283-90

32. Baldocchi DD, Hicks BB, Meyers TP. 1988. Measuring biosphere-atmosphere exchanges of biologically related gases with micrometeorological methods. *Ecology* 69:1331-40
33. Pryor S, Larsen SE, Sørensen LL, Barthelmie RJ, Grönholm T, et al. 2007. Particle fluxes over forests: Analyses of flux methods and functional dependencies. *Journal of Geophysical Research: Atmospheres* 112
34. Baldocchi DD. 2003. Assessing the eddy covariance technique for evaluating carbon dioxide exchange rates of ecosystems: past, present and future. *Global Change Biol* 9:479-92
35. Rizzo LV, Artaxo P, Karl T, Guenther AB, Greenberg J. 2010. Aerosol properties, in-canopy gradients, turbulent fluxes and VOC concentrations at a pristine forest site in Amazonia. *Atmos Environ* 44:503-11
36. Ahlm L, Krejci R, Nilsson ED, Martensson EM, Vogt M, Artaxo P. 2010. Emission and dry deposition of accumulation mode particles in the Amazon Basin. *Atmos Chem Phys* 10:10237-53
37. Farmer DK, Kimmel JR, Phillips G, Docherty KS, Worsnop DR, et al. 2011. Eddy covariance measurements with high-resolution time-of-flight aerosol mass spectrometry: a new approach to chemically resolved aerosol fluxes. *Atmos Meas Tech* 4:1275-89
38. Nemitz E, Jimenez JL, Huffman JA, Ulbrich IM, Canagaratna MR, et al. 2008. An eddy-covariance system for the measurement of surface/atmosphere exchange fluxes of submicron aerosol chemical species - First application above an urban area. *Aerosol Sci Tech* 42:636-57
39. Lavi A, Farmer DK, Segre E, Moise T, Rotenberg E, et al. 2013. Fluxes of Fine Particles Over a Semi-Arid Pine Forest: Possible Effects of a Complex Terrain. *Aerosol Sci Tech* 47:906-15
40. Gaman A, Rannik Ü, Aalto P, Pohja T, Siivola E, et al. 2004. Relaxed Eddy Accumulation System for Size-Resolved Aerosol Particle Flux Measurements. *J Atmos Ocean Tech* 21:933-43
41. Gaman A, Rannik U, Aalto P, Pohja T, Siivola E, et al. 2004. Relaxed eddy accumulation system for size-resolved aerosol particle flux measurements. *J Atmos Ocean Tech* 21:933-43
42. Schery SD, Wasiolek PT, Nemetz BM, Yarger FD, Whittlestone S. 1998. Relaxed eddy accumulator for flux measurement of nanometer-size particles. *Aerosol Sci Tech* 28:159-72
43. Pryor SC, Larsen SE, Sørensen LL, Barthelmie RJ. 2008. Particle fluxes above forests: Observations, methodological considerations and method comparisons. *Environmental Pollution* 152:667-78
44. Held A, Niessner R, Bosveld F, Wrzesinsky T, Klemm O. 2007. Evaluation and Application of an Electrical Low Pressure Impactor in Disjunct Eddy Covariance Aerosol Flux Measurements. *Aerosol Sci Tech* 41:510-9
45. Held A, Hinz K-P, Trimborn A, Spengler B, Klemm O. 2003. Towards direct measurement of turbulent vertical fluxes of compounds in atmospheric aerosol particles. *Geophys Res Lett* 30
46. Pryor S, Barthelmie RJ, Sørensen LL, Larsen SE, Sempreviva AM, et al. 2008. Upward fluxes of particles over forests: when, where, why? *Tellus B: Chemical and Physical Meteorology* 60:372-80
47. Buzorius G, Rannik U, Makela JM, Vesala T, Kulmala M. 1998. Vertical aerosol particle fluxes measured by eddy covariance technique using condensational particle counter. *J Aerosol Sci* 29:157-71

48. Märtensson EM, Nilsson ED, Buzorius G, Johansson C. 2006. Eddy covariance measurements and parameterisation of traffic related particle emissions in an urban environment. *Atmos Chem Phys* 6:769-85
49. Nemitz E, Sutton MA. 2004. Gas-particle interactions above a Dutch heathland: III. Modelling the influence of the NH3-HNO3-NH4NO3 equilibrium on size-segregated particle fluxes. *Atmos Chem Phys* 4:1025-45
50. Trebs I, Lara LL, Zeri LMM, Gatti LV, Artaxo P, et al. 2006. Dry and wet deposition of inorganic nitrogen compounds to a tropical pasture site (Rondonia, Brazil). *Atmos Chem Phys* 6:447-69
51. Farmer DK, Chen Q, Kimmel JR, Docherty KS, Nemitz E, et al. 2013. Chemically resolved particle fluxes over tropical and temperate forests. *Aerosol Sci Tech* 47:818-30
52. Pryor SC, Binkowski FS. 2004. An Analysis of the Time Scales Associated with Aerosol Processes during Dry Deposition. *Aerosol Sci Tech* 38:1091-8
53. Petroff A, Mailliat A, Amielh M, Anselmet F. 2008. Aerosol dry deposition on vegetative canopies. Part I: review of present knowledge. *Atmos Environ* 42:3625-53
54. Petroff A, Zhang L. 2010. Development and validation of a size-resolved particle dry deposition scheme for application in aerosol transport models. *Geosci Model Dev* 3:753
55. Petroff A, Mailliat A, Amielh M, Anselmet F. 2008. Aerosol dry deposition on vegetative canopies. Part II: A new modelling approach and applications. *Atmos Environ* 42:3654-83
56. Sievering H. 1987. Small-particle dry deposition under high wind speed conditions: Eddy flux measurements at the boulder atmospheric observatory. *Atmospheric Environment (1967)* 21:2179-85
57. GröNholm T, Aalto PP, Hiltunen VJ, Rannik Ü, Rinne J, et al. 2007. Measurements of aerosol particle dry deposition velocity using the relaxed eddy accumulation technique. *Tellus B: Chemical and Physical Meteorology* 59:381-6
58. Wesely ML. 1989. Parameterization of surface resistances to gaseous dry deposition in regional-scale numerical models. *Atmos Environ* 23:1293-304
59. Peters K, Eiden R. 1992. Modeling the Dry Deposition Velocity of Aerosol-Particles to a Spruce Forest. *Atmos Environ a-Gen* 26:2555-64
60. Giardina M, Buffa P. 2018. A new approach for modeling dry deposition velocity of particles. *Atmos Environ* 180:11-22
61. Giorgi F. 1986. A Particle Dry-Deposition Parameterization Scheme for Use in Tracer Transport Models. *J Geophys Res-Atmos* 91:9794-806
62. GIORGI F. 1988. Dry deposition velocities of atmospheric aerosols as inferred by applying a particle dry deposition parameterization to a general circulation model. *Tellus B* 40B:23-41
63. Pleim J, Ran L. 2011. Surface flux modeling for air quality applications. *Atmosphere* 2:271-302
64. Fairall CW. 2004. Title. Volume:In press
65. Fairall CW, Hare JE, Edson JB, McGillis W. 2000. Parameterization and micrometeorological measurement of air-sea gas transfer. *Bound-Lay Meteorol* 96:63-105
66. Sievering H. 1984. Small-Particle Dry Deposition on Natural-Waters - Modeling Uncertainty. *J Geophys Res-Atmos* 89:9679-81
67. Slinn SA, Slinn WGN. 1980. Predictions for Particle Deposition on Natural-Waters. *Atmos Environ* 14:1013-6
68. Williams RM. 1982. A Model for the Dry Deposition of Particles to Natural-Water Surfaces. *Atmos Environ* 16:1933-8
69. Pryor SC, Barthelmie RJ. 2000. Particle dry deposition to water surfaces: Processes and consequences. *Mar Pollut Bull* 41:220-31

70. Emerson EW, Katich JM, Schwarz JP, McMeeking GR, Farmer DK. 2018. Direct Measurements of Dry and Wet Deposition of Black Carbon Over a Grassland. *J Geophys Res-Atmos* 123:12277-90
71. Warren SG, Wiscombe WJ. 1980. A model for the spectral albedo of snow. II: Snow containing atmospheric aerosols. *J Atmos Sci* 37:2734-45
72. Flanner MG, Zender CS, Randerson JT, Rasch PJ. 2007. Present-day climate forcing and response from black carbon in snow. *Journal of Geophysical Research: Atmospheres* 112
73. Koch D, Del Genio A. 2010. Black carbon semi-direct effects on cloud cover: review and synthesis. *Atmos Chem Phys* 10:7685-96
74. Hansen J, Nazarenko L. 2004. Soot climate forcing via snow and ice albedos. *Proceedings of the National Academy of Sciences* 101:423-8
75. Bond TC, Streets DG, Yarber KF, Nelson SM, Woo JH, Klimont Z. 2004. A technology-based global inventory of black and organic carbon emissions from combustion. *Journal of Geophysical Research: Atmospheres* 109
76. Hadley OL, Corrigan CE, Kirchstetter TW, Cliff SS, Ramanathan V. 2010. Measured black carbon deposition on the Sierra Nevada snow pack and implication for snow pack retreat. *Atmos Chem Phys* 10:7505-13
77. Kaspari S, Skiles SM, Delaney I, Dixon D, Painter TH. 2015. Accelerated glacier melt on Snow Dome, Mount Olympus, Washington, USA, due to deposition of black carbon and mineral dust from wildfire. *J Geophys Res-Atmos* 120:2793-807
78. Menon S, Koch D, Beig G, Sahu S, Fasullo J, Orlikowski D. 2010. Black carbon aerosols and the third polar ice cap. *Atmos Chem Phys* 10:4559-71
79. Yasunari TJ, Tan Q, Lau KM, Bonasoni P, Marinoni A, et al. 2013. Estimated range of black carbon dry deposition and the related snow albedo reduction over Himalayan glaciers during dry pre-monsoon periods. *Atmos Environ* 78:259-67
80. Mahmood R, von Salzen K, Flanner M, Sand M, Langner J, et al. 2016. Seasonality of global and Arctic black carbon processes in the Arctic Monitoring and Assessment Programme models. *Journal of Geophysical Research: Atmospheres* 121:7100-16
81. Schwarz JP, Gao RS, Fahey DW, Thomson DS, Watts LA, et al. 2006. Single-particle measurements of midlatitude black carbon and light-scattering aerosols from the boundary layer to the lower stratosphere. *J Geophys Res-Atmos* 111
82. Stephens M, Turner N, Sandberg J. 2003. Particle identification by laser-induced incandescence in a solid-state laser cavity. *Appl Optics* 42:3726-36
83. Joshi R, Liu D, Nemitz E, Langford B, Mullinger N, et al. 2020. Direct measurements of black carbon fluxes in central Beijing using the eddy-covariance method. *Atmos. Chem. Phys. Discuss.* 2020:1-27
84. Andrews T, Gregory JM, Webb MJ, Taylor KE. 2012. Forcing, feedbacks and climate sensitivity in CMIP5 coupled atmosphere-ocean climate models. *Geophys Res Lett* 39:Doi 10.1029/2012gl051607
85. Bony S, Dufresne JL. 2005. Marine boundary layer clouds at the heart of tropical cloud feedback uncertainties in climate models. *Geophys Res Lett* 32:Doi 10.1029/2005gl023851
86. Twomey S. 1974. Pollution and Planetary Albedo. *Atmos Environ* 8:1251-6
87. Ackerman AS, Toon OB, Taylor JP, Johnson DW, Hobbs PV, Ferek RJ. 2000. Effects of aerosols on cloud albedo: Evaluation of Twomey's parameterization of cloud susceptibility using measurements of ship tracks. *J Atmos Sci* 57:2684-95
88. Contini D, Donateo A, Belosi F, Grasso F, Santachiara G, Prodi F. 2010. Deposition velocity of ultrafine particles measured with the Eddy-Correlation Method over the Nansen Ice Sheet (Antarctica). *Journal of Geophysical Research: Atmospheres* 115

89. Duan B, Fairall C, Thomson D. 1988. Eddy correlation measurements of the dry deposition of particles in wintertime. *J Appl Meteorol* 27:642-52
90. Ibrahim M, Barrie L, Fanaki F. 1983. An experimental and theoretical investigation of the dry deposition of particles to snow, pine trees and artificial collectors. *Atmospheric Environment (1967)* 17:781-8
91. Nilsson ED, Rannik Ü. 2001. Turbulent aerosol fluxes over the Arctic Ocean: 1. Dry deposition over sea and pack ice. *Journal of Geophysical Research: Atmospheres* 106:32125-37
92. Grönlund A, Nilsson D, Koponen IK, Virkkula A, Hansson ME. 2002. Aerosol dry deposition measured with eddy-covariance technique at Wasa and Aboa, DronningMaud Land, Antarctica. *Annals of Glaciology* 35:355-61
93. Gallagher M, Beswick K, Choularton T. 1992. Measurement and modelling of cloudwater deposition to a snow-covered forest canopy. *Atmospheric Environment. Part A. General Topics* 26:2893-903
94. Macdonald KM, Sharma S, Toom D, Chivulescu A, Hanna S, et al. 2017. Observations of atmospheric chemical deposition to high Arctic snow.
95. Huang L, Gong SL, Jia CQ, Lavoue D. 2010. Importance of deposition processes in simulating the seasonality of the Arctic black carbon aerosol. *J Geophys Res-Atmos* 115
96. Tammet H, Kimmel V, Israelsson S. 2001. Effect of atmospheric electricity on dry deposition of airborne particles from atmosphere. *Atmos Environ* 35:3413-9
97. Pryor SC, Barthelmie RJ, Larsen SE, Sørensen LL. 2017. Ultrafine particle number fluxes over and in a deciduous forest. *Journal of Geophysical Research: Atmospheres* 122:405-22
98. Rannik U, Mammarella I, Aalto P, Keronen P, Vesala T, Kulmala M. 2009. Long-term aerosol particle flux observations part I: Uncertainties and time-average statistics. *Atmos Environ* 43:3431-9
99. Mammarella I, Rannik Ü, Aalto P, Keronen P, Vesala T, Kulmala M. 2011. Long-term aerosol particle flux observations. Part II: Particle size statistics and deposition velocities. *Atmos Environ* 45:3794-805
100. Deventer MJ, von der Heyden L, Lamprecht C, Graus M, Karl T, Held A. 2018. Aerosol particles during the Innsbruck Air Quality Study (INNAQS): Fluxes of nucleation to accumulation mode particles in relation to selective urban tracers. *Atmos Environ* 190:376-88
101. Jarvi L, Rannik U, Mammarella I, Sogachev A, Aalto PP, et al. 2009. Annual particle flux observations over a heterogeneous urban area. *Atmos Chem Phys* 9:7847-56
102. Conte M, Contini D. 2019. Size-resolved particle emission factors of vehicular traffic derived from urban eddy covariance measurements. *Environmental Pollution* 251:830-8
103. Pallozzi E, Guidolotti G, Mattioni M, Calfapietra C. 2020. Particulate matter concentrations and fluxes within an urban park in Naples. *Environmental Pollution* 266:115134
104. Fares S, Savi F, Fusaro L, Conte A, Salvatori E, et al. 2016. Particle deposition in a peri-urban Mediterranean forest. *Environmental Pollution* 218:1278-86
105. Ahlm L, Nilsson ED, Krejci R, Martensson EM, Vogt M, Artaxo P. 2009. Aerosol number fluxes over the Amazon rain forest during the wet season. *Atmos Chem Phys* 9:9381-400
106. Chamberlain A. 1967. Transport of Lycopodium spores and other small particles to rough surfaces. *Proceedings of the Royal Society of London. Series A. Mathematical and Physical Sciences* 296:45-70
107. Clough W. 1975. The deposition of particles on moss and grass surfaces. *Atmospheric Environment (1967)* 9:1113-9

108. Wesely M, Hicks B, Dannevik W, Frisella S, Husar R. 1977. An eddy-correlation measurement of particulate deposition from the atmosphere. *Atmospheric Environment (1967)* 11:561-3
109. Garland J, Cox L. 1982. Deposition of small particles to grass. *Atmospheric Environment (1967)* 16:2699-702
110. Dollard G, Unsworth M. 1983. Field measurements of turbulent fluxes of wind-driven fog drops to a grass surface. *Atmospheric Environment (1967)* 17:775-80
111. Katen PC, Hubbe JM. 1985. An evaluation of optical particle counter measurements of the dry deposition of atmospheric aerosol particles. *Journal of Geophysical Research: Atmospheres* 90:2145-60
112. Wesely M, Cook D, Hart R, Speer R. 1985. Measurements and parameterization of particulate sulfur dry deposition over grass. *Journal of Geophysical Research: Atmospheres* 90:2131-43
113. Hicks B, Wesely M, Coulter R, Hart R, Durham J, et al. 1986. An experimental study of sulfur and NO x fluxes over grassland. *Bound-Lay Meteorol* 34:103-21
114. Gallagher M, Choularton T, Morse A, Fowler D. 1988. Measurements of the size dependence of cloud droplet deposition at a hill site. *Q J Roy Meteor Soc* 114:1291-303
115. Fowler D, Morse A, Gallagher M, Choularton T. 1990. Measurements of cloud water deposition on vegetation using a lysimeter and a flux gradient technique. *Tellus B* 42:285-93
116. Allen A, Harrison R, Nicholson K. 1991. Dry deposition of fine aerosol to a short grass surface. *Atmospheric Environment. Part A. General Topics* 25:2671-6
117. Nemitz E, Gallagher MW, Duyzer JH, Fowler D. 2002. Micrometeorological measurements of particle deposition velocities to moorland vegetation. *Quarterly Journal of the Royal Meteorological Society: A journal of the atmospheric sciences, applied meteorology and physical oceanography* 128:2281-300
118. Vong RJ, Vickers D, Covert DS. 2004. Eddy correlation measurements of aerosol deposition to grass. *Tellus B: Chemical and Physical Meteorology* 56:105-17
119. Connan O, Pellerin G, Maro D, Damay P, Hébert D, et al. 2018. Dry deposition velocities of particles on grass: Field experimental data and comparison with models. *J Aerosol Sci* 126:58-67
120. Höfken KD, Gravenhorst G. 1982. Deposition of atmospheric aerosol particles to beech- and spruce forest. In *Deposition of atmospheric pollutants*:191-4: Springer. Number of 191-4 pp.
121. Grosch S, Schmitt G. 1988. Experimental investigations on the deposition of trace elements in forest areas. In *Environmental Meteorology*:201-16: Springer. Number of 201-16 pp.
122. Waraghai A, Gravenhorst G. 1989. Dry Deposition of Atmoshperic Particles to an Old Spruce Stand. In *Mechanisms and Effects of Pollutant-transfer into Forests*:77-86: Springer. Number of 77-86 pp.
123. Lorenz R, Murphy C. 1989. Dry deposition of particles to a pine plantation. *Bound-Lay Meteorol* 46:355-66
124. Gallagher M, Beswick K, Duyzer J, Westrate H, Choularton T, Hummelshøj P. 1997. Measurements of aerosol fluxes to Speulder forest using a micrometeorological technique. *Atmos Environ* 31:359-73
125. Held A, Nowak A, Wiedensohler A, Klemm O. 2006. Field measurements and size-resolved model simulations of turbulent particle transport to a forest canopy. *J Aerosol Sci* 37:786-98
126. Pryor S. 2006. Size-resolved particle deposition velocities of sub-100 nm diameter particles over a forest. *Atmos Environ* 40:6192-200

127. Grönholm T, Launiainen S, Ahlm L, Mårtensson E, Kulmala M, et al. 2009. Aerosol particle dry deposition to canopy and forest floor measured by two-layer eddy covariance system. *Journal of Geophysical Research: Atmospheres* 114
128. Gordon M, Staebler RM, Liggio J, Vlasenko A, Li SM, Hayden K. 2011. Aerosol flux measurements above a mixed forest at Borden, Ontario. *Atmos Chem Phys* 11:6773-86
129. Zhang J, Shao Y, Huang N. 2014. Measurements of dust deposition velocity in a wind-tunnel experiment. *Atmos. Chem. Phys.* 14:8869-82
130. Deventer MJ, Held A, El-Madany TS, Klemm O. 2015. Size-resolved eddy covariance fluxes of nucleation to accumulation mode aerosol particles over a coniferous forest. *Agr Forest Meteorol* 214-215:328-40
131. Möller U, Schumann G. 1970. Mechanisms of transport from the atmosphere to the Earth's surface. *J Geophys Res* 75:3013-9
132. Sehmel G, Sutter S, Simpson C. 1974. Particle deposition rates on a water surface as a function of particle diameter and air velocity, Battelle Pacific Northwest Labs., Richland, Wash.(USA)
133. Larsen SE, Edson J, Hummelshøj P, Jensen NO, De Leeuw G, Mestayer P. 1995. Dry deposition of particles to ocean surfaces. *Ophelia* 42:193-204
134. Gustafsson ME, Franzén LG. 1996. Dry deposition and concentration of marine aerosols in a coastal area, SW Sweden. *Atmos Environ* 30:977-89
135. Zufall MJ, Davidson CI, Caffrey PF, Ondov JM. 1998. Airborne concentrations and dry deposition fluxes of particulate species to surrogate surfaces deployed in southern Lake Michigan. *Environ Sci Technol* 32:1623-8
136. Caffrey PF, Ondov JM, Zufall MJ, Davidson CI. 1998. Determination of size-dependent dry particle deposition velocities with multiple intrinsic elemental tracers. *Environ Sci Technol* 32:1615-22
137. Petelski T. 2003. Marine aerosol fluxes over open sea calculated from vertical concentration gradients. *J Aerosol Sci* 34:359-71
138. Pryor S, Gallagher M, Sievering H, Larsen SE, Barthelmie RJ, et al. 2008. A review of measurement and modelling results of particle atmosphere–surface exchange. *Tellus B: Chemical and Physical Meteorology* 60:42-75
139. Zhang G, Zhang J, Liu S. 2007. Characterization of nutrients in the atmospheric wet and dry deposition observed at the two monitoring sites over Yellow Sea and East China Sea. *J Atmos Chem* 57:41-57
140. Shi J-H, Zhang J, Gao H-W, Tan S-C, Yao X-H, Ren J-L. 2013. Concentration, solubility and deposition flux of atmospheric particulate nutrients over the Yellow Sea. *Deep Sea Research Part II: Topical Studies in Oceanography* 97:43-50
141. Calec N, Boyer P, Anselmet F, Amielh M, Branger H, Mailliat A. 2017. Dry deposition velocities of submicron aerosols on water surfaces: Laboratory experimental data and modelling approach. *J Aerosol Sci* 105:179-92
142. Qi J, Yu Y, Yao X, Gang Y, Gao H. 2020. Dry deposition fluxes of inorganic nitrogen and phosphorus in atmospheric aerosols over the Marginal Seas and Northwest Pacific. *Atmos Res*:105076

Figures and Tables

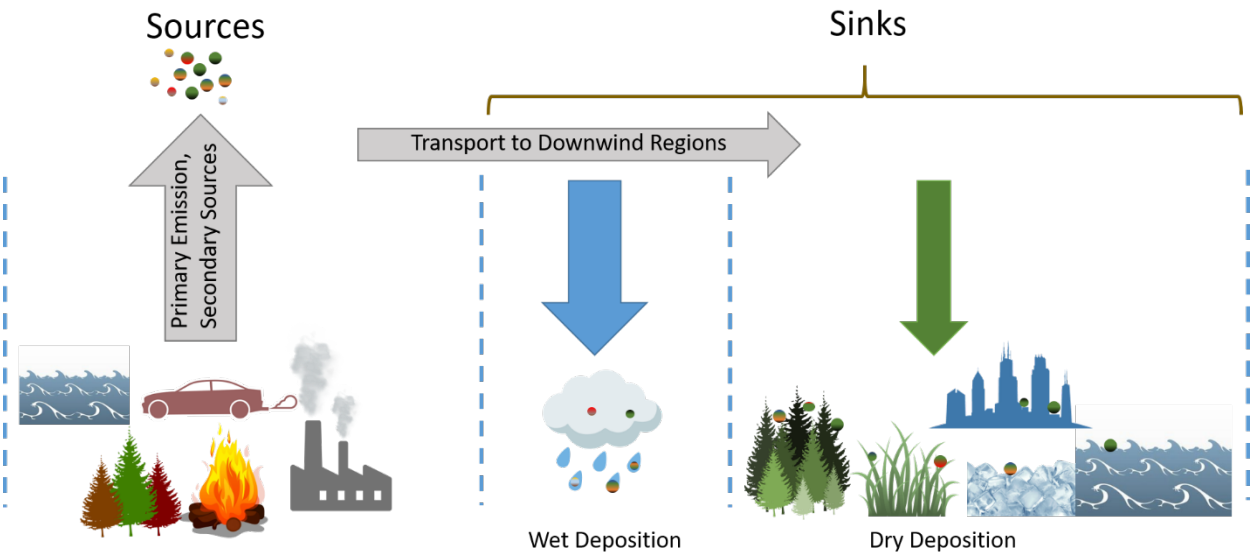

Figure 1: Primary emissions and secondary chemistry are key sources of aerosols in the atmosphere. Wet deposition and dry deposition remove particles, determining the lifetime of aerosols in the atmosphere. Deposition surfaces include forests, grasslands, ice, water and urban environments, with each surface type removing particles at different size-dependent and turbulence-dependent rates.

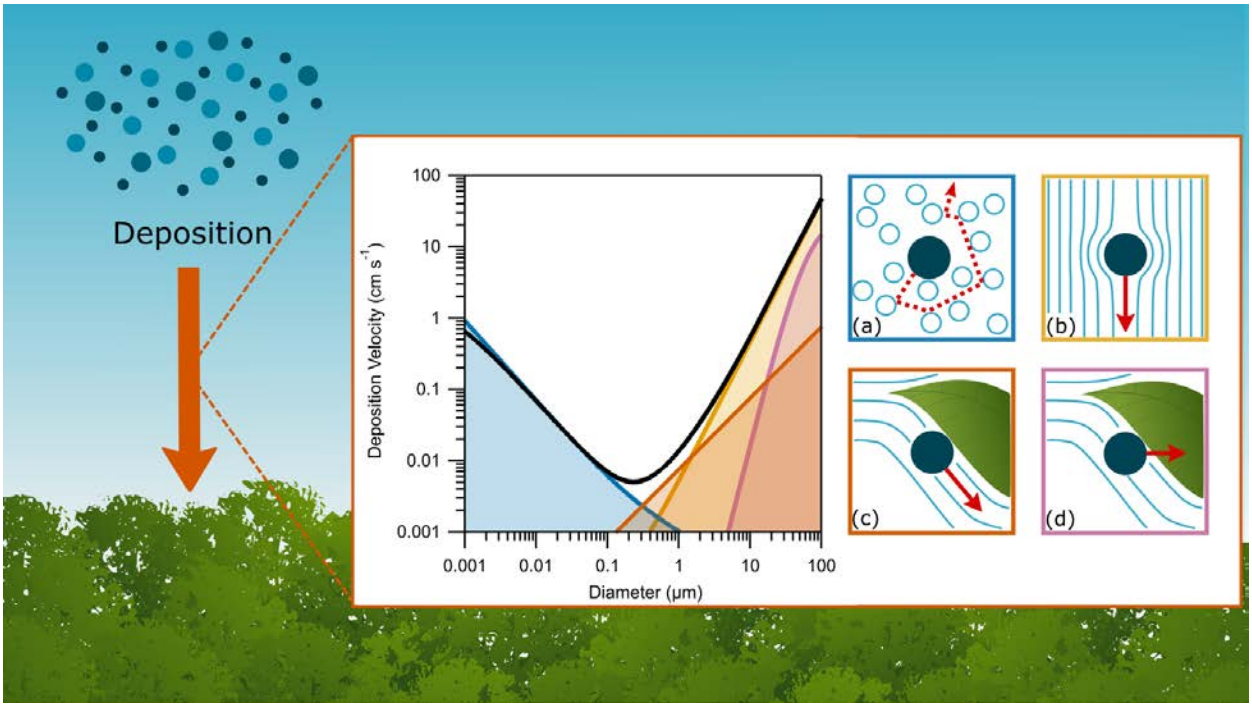

Figure 2: Dry deposition velocities of particles are a function of particle diameter, and driven by a combination of processes including Brownian diffusion (a, blue), gravitational settling (b, yellow), interception (c, orange), and impaction (d, pink). The relative importance of these processes varies with particle size and surface type.

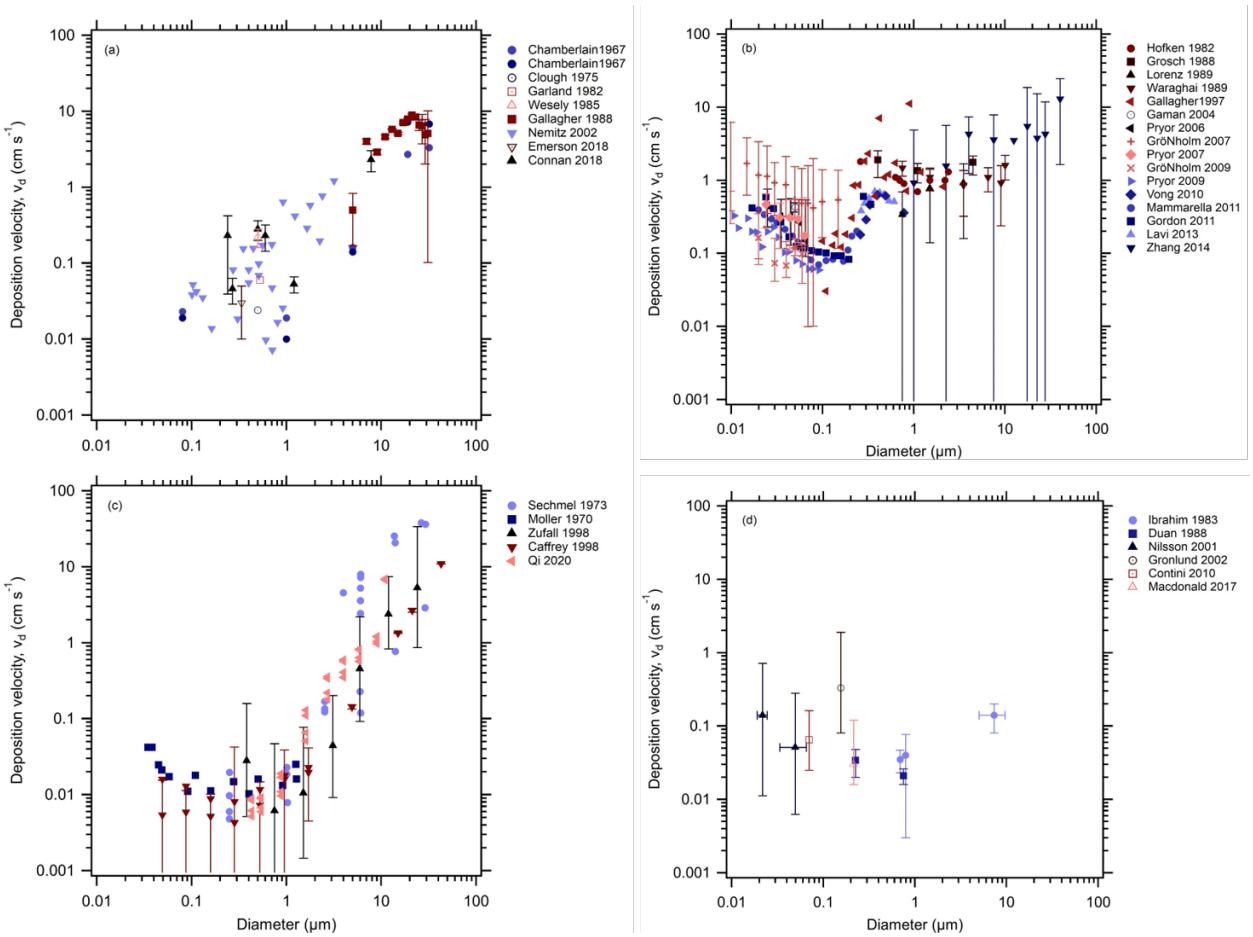

Figure 3. Compilations of multiple size-resolved particle flux observations as deposition velocity as a function of size over grasslands (a), forests (b), water surfaces (c) and the cryosphere (d). These datasets are not normalized for friction velocity (u*), which is established to strongly influence flux.

Table 1. Size-resolved particle flux observations, separated by land use type, method, size range and typical deposition velocity. We exclude urban fluxes (see Section 6.3).

Land Use Type	Site Location and Details	Method	Size Range (μm)	V_{dep} (cm/s)	Study
Grass	Grass and Filter paper	Gradient	0.08 – 32	0.01 – 7.2	Chamberlain and Spence 1967 (106)
	Moss (*Hypnum cupressiforme)* and Italian rye grass	Wind tunnel experiment	0.5	0.024	Clough 1975 (107)
	Wood River refinery com-plex Illinois, USA	Eddy covariance	0.05 – 0.1	0.6 ± 0.4	Wesely et al. 1977 (108)
	Grass	Gradient	0.05 – 1	0.525	Garland and Cox 1982 (109)
	Mount St. Bernard Abbey near Coalville, Leicestershire, England	Gradient	5 – 30	2.4 – 7.0	Dollard and Unsworth 1983 (110)
	Champaign Illinois, USA	Eddy covariance	0.15 – 2.5	Negative	Katen and Hubbe 1985 (111)
	Champaign Illinois, USA	Eddy covariance	~ 0.1 – 1	0.22 ± 0.06	Wesely et al. 1985 (112)
	South Charleston Ohio, USA	Eddy covariance	< 1	0.4 – 0.8	Hicks et al. 1986 (113)
	Great Dun Fell, England Moorland with Eriophorun and Juncus species	Gradient	5 – 31	0.5 – 8.9	Gallagher et al. 1988 (114)
	Great Dun Fell, England Moorland with *Eriophorun* and *Juncus* species	Gradient	2 – 30	2.1 – 3.9	Fowler et al. 1990 (115)
	Sport fields at the University of Essex Colchester, England	Gradient	0.1 – 2	0.10 ± 0.03	Allen et al. 1991 (116)

	Auchencorth Moss field site, South East Scotland Transitional lowland raised bog, *Sphagnum* species	Eddy covariance	0.1 – 3	0.007 – 1.2	Nemitz et al. 2002 (117)
	Shedd, Oregon Field of rye grass	Eddy covariance	0.52	0.16 – 0.44	Vong et al. 2004 (118)
	Southern Great Plains (SGP) site Lamont, Oklahoma, USA Alfalfa (*Medicago sativa*) field	Eddy covariance	0.07 – 0.6	0.03 ± 0.02	Emerson et al. 2018 (70)
	Grass cuttings and synthetic commercial grass	Gradient	0.24 – 7.8	0.046 – 2.3	Connan et al. 2018 (119)
Forest					
	Solling forest (Spruce and beech trees)	Gradient	0.26 – 2.4	0.7 – 1.8	Hofken 1982 (120)
	Königstein Frankfurt, Germany	Gradient	0.1 – 10	1.4 – 1.9	Grosch and Schmitt 1988 (121)
	Spruce forest	Gradient	0.5 – 10	0.8 – 1.6	Waraghai et al. 1989 (122)
	Pine plantation	Gradient	0.5 – 5	0.34 – 0.92	Lorenz and Murphy 1989 (123)
	Speulderbos Holland, Netherlands Douglas fir forest	Eddy covariance	0.1 - 3	0.02 - 11	Gallagher 1997 (124)
	Scots Pine forest (SMEAR II station), Hyytiäälä Finland	Eddy covariance	0.012 – 1		Buzorius et al. 1998 (47)
	Scots Pine forest (SMEAR II station), Hyytiäälä Finland	REA	0.05	0.43 ± 0.06	Gaman et al. 2004 (40)
	Norway spruce forest (Waldstein	Eddy covariance	0.003 – 0.8	-0.23 - 0.37	Held et al. 2006 (125)

	research site, Germany)				
	CarboEuroFlux experimental forest site Sorø, Denmark Beech forest	Eddy covariance	0.02 – 0.07	0.15 – 0.45	Pryor et al. 2006 (126)
	Scots Pine forest (SMEAR II station), Hyytiäälä Finland	REA	0.008 – 0.15	0.6-2.1	GröNholm et al. 2007 (57)
	Sorø, Denmark Beech forest & Scots Pine forest (SMEAR II station), Hyytiälä, Finland	Eddy covariance and REA	0.01 – 0.1	0.2 – 0.5	Pryor et al. 2007 (33)
	Reserva Biológica do Cuieiras Manaus, Brazil	Eddy covariance	0.01 – 0.1		Ahlm 2009 (105)
	Scots Pine forest (SMEAR II station), Hyytiälä, Finland	Eddy covariance	0.01 – 0.06	0.06 – 0.5	GröNholm et al. 2009 (127)
	Morgan-Monroe State Forest (MMSF) Indiana, USA Mixed deciduous: sugar maple, tulip poplar, sassafras, white oak, and black oak	Eddy covariance	0.008 – 0.1	0.06 – 0.3	Pryor et al. 2009 (10)
	Wet tropical rainforest (Amazonia, Brazil)	Eddy covariance	0.25-2.5		Ahlm et al. 2010 (36)
	Cuieiras Manaus, Brazil	Eddy covariance	0.01 – 0.3	Reports flux	Rizzo et al. 2010 (35)
	Ponderosa pine plantation	Eddy covariance	0.25 – 1.0	0.2-0.6	Vong et al. 2010 (11)
	Borden Forest Research Station Ontario, Canada	Eddy covariance	0.018 – 0.452	0.08 – 0.6	Gordon et al. 2011 (128)

	Mix of hardwood and coniferous trees				
	SMEAR II station Hyytiälä, Southern Finland Scots pine forest	Eddy covariance	0.01 – 0.3	0.07 – 0.4	Mammarella et al. 2011 (99)
	Yatir Forest Research Station, Israel Aleppo pine trees	Eddy covariance	0.25 – 0.65		Lavi et al. 2013 (39)
	Lab	Wind tunnel experiment	0.5 – 200	0.9 - 13	Zhang 2014 (129)
	Norway spruce forest (Waldstein research site, Germany)	Eddy covariance	0.006 – 1.4	-0.27	Deventer et al. 2015 (130)
	Ontario, Canada Temperate broadleaf forest	Eddy covariance	0.05 – 0.5		Petroff et al. 2018 (12)
Water	Lab	Wind tunnel experiments	0.04 – 1.5	0.01 – 0.04	Möller and Schumann 1970 (131)
	Lab	Wind tunnel experiments	0.3 – 28	0.004 – 38	Sehmel and Sutter 1974 (132)
	Lab	Wind tunnel experiments	0.1 - 1		Larsen et al. 1995 (133)
	Southwest coast of Sweden, near Falkenberg	Gradient	0.05 – 10		Gustafsson and Franzen 1996 (134)
	Lake Michigan	Gradient	0.25 – 100	0.06 – 5	Zufall et al. 1998 (135)
	Lake Michigan	Physical sampling	0.05 – 50	0.004 – 11	Caffrey et al. 1998 (136)
	Baltic Sea	Gradient	1 – 20	Only report flux	Petelski 2003 (137)
	Surf zone on the island of Østergarnsholm, Sweden	Physical sampling	0.5 – 20		Pryor et al. 2008 (138)
	Northwest Pacific Ocean: The Yellow Sea and	Physical sampling	~0.5 – 35		Zhang et al. 2007 (139)

	the East China Sea				
	Yellow Sea	Physical sampling	~0.5 – 11		Shi et al. 2013 (140)
	Lab	Wind tunnel experiments		$6x10^{-5}$ – 0.004	Calec et al. 2017 (141)
	Marginal Seas of China (Yellow Sea, Bohai Sea, East China Sea, and South China Sea) and the Northwest Pacific Ocean	Physical sampling	~0.5 – 11	0.0052 – 6.97	Qi et al. 2020 (142)
Snow and Ice	Snow field	Physical sampling	0.7 – 7	0.035 – 0.14	Ibrahim et al. 1983 (90)
	Pennsylvania State University Agricultural Research Farm Rock Springs, PA Snow covered field	Eddy covariance	0.15 – 1	0.021 – 0.034	Duan et al. 1988 (89)
	Dunslair Hights, Scotland Snow covered Sitka spruce forest	Eddy covariance	3 – 31	- 4.4 – 50.9	Gallagher et al. 1992 (93)
	Arctic Ocean Ice floe	Eddy covariance	0.01 – 1	0.05 – 0.14	Nilsson and Rannik 2001 (91)
	Dronning Maud Land (DML), Antarctica Smooth snow surface	Eddy covariance	0.01 – 0.85	0.08 – 1.89	Grönlund et al. 2002 (92)
	Nansen Ice Sheet, Antarctica Iced branch of the Ross Sea	Eddy covariance	0.01 - 1	0.06 ± 0.09	Contini et al. 2010 (88)
	Neil Trivett Global Atmosphere Watch Observatory Alert, Nunavut	Physical sampling	0.07 – 0.5	0.03 ± 0.09	Macdonald et al. 2017 (94)